

1 Separable roles for RanGTP in nuclear and 2 ciliary trafficking of a kinesin-2 subunit

3 Shengping Huang ^{2*} and Prachee Avasthi ^{1,2*}

4
5 ¹ Anatomy and Cell Biology, University of Kansas Medical Center, Kansas City, KS; ² Ophthalmology,
6 University of Kansas Medical Center, Kansas City, KS. *Addresses for correspondence: Shengping
7 Huang (E-mail address: sphalan@gmail.com); Prachee Avasthi (Email address: pavasthi@kumc.edu)
8

9 **Abstract**

10 Kinesin is part of the microtubule (MT)-binding motor protein superfamily, which exerts crucial
11 functions in cell division and intracellular transport in different organelles. The heterotrimeric
12 kinesin-2, consisting of the kinesin like protein KIF3A/3B heterodimer and kinesin-associated
13 protein KAP3, is highly conserved across species from the green alga *Chlamydomonas* to
14 humans. It plays diverse roles in cargo transport including anterograde (base to tip) trafficking in
15 cilium. However, the molecular determinants mediating trafficking of heterotrimeric kinesin-2
16 itself is poorly understood. Using the unicellular eukaryote *Chlamydomonas* and mammalian
17 cells, we show that RanGTP regulates ciliary trafficking of KAP3. We found the armadillo repeat
18 region 6-9 (ARM6-9) of KAP3, required for its nuclear translocation, is sufficient for its targeting
19 to the ciliary base. Given that KAP3 is essential for cilia formation and the emerging roles of
20 RanGTP/importin β in ciliary protein targeting, we further investigate the effect of RanGTP in
21 cilium length regulation in these two different systems. We demonstrate that precise control of
22 RanGTP levels, revealed by different Ran mutants, is crucial for cilium formation and
23 maintenance. Most importantly, we were able to segregate RanGTP regulation of ciliary protein
24 incorporation from of its nuclear roles. Our work provides important support for the model that
25 nuclear import mechanisms have been coopted for independent roles in ciliary import.
26

27 **Key words:** RanGTP, Kinesin-2, KAP3, nuclear import, ciliary targeting
28
29

30 **Introduction**

31 Cilia are microtubule-based protrusions with sensory and/or motile functions. In mammals,
32 defects in assembly and maintenance of cilia results in a series of diseases called “ciliopathies”

33 (Fliegau et al., 2007; Mitchison et al., 2017; Anvarian et al., 2019; Breslow et al., 2019). The
34 assembly and maintenance of these organelles are dependent on anterograde and retrograde
35 intraflagellar transport (IFT) (Rosenbaum et al., 2002). Anterograde IFT, which moves from the
36 base of a cilium to the tip, is driven by kinesin-2 (Kozminski et al., 1995; Cole et al., 1998),
37 whereas retrograde IFT, which moves from the tip back to the base, is achieved by cytoplasmic
38 dynein 1b (Signor et al., 1999; Pazour et al., 1999; Porter et al., 1999). The kinesin-2 motor
39 family is composed of a heterotrimeric KIF3A/KIF3B/KAP3 motor and a homodimeric KIF17
40 motor (Hirokawa et al. 2009). Unlike homodimeric KIF17, heterotrimeric kinesin-2 is highly
41 conserved, and loss of function in any component of heterotrimeric kinesin-2 results in defective
42 cilia in different organisms (Walther et al., 1994; Morris et al., 1997; Sarpal et al., 2004; Zhao et
43 al., 2011). In addition to cilium formation, regulation and maintenance of cilium length is also
44 dependent on the size and frequency of kinesin-2 trains recruited to/entering cilia (Ludington et
45 al., 2013; Engel et al., 2009). In addition to its central role in IFT and ciliogenesis, heterotrimeric
46 kinesin-2 has also been reported in other organelle transport events outside cilia. This includes
47 anterograde transport from endoplasmic reticulum to the Golgi apparatus in *Xenopus* (Le Bot et
48 al., 1998), retrograde transport from the Golgi to endoplasmic reticulum in HeLa cells (Stauber
49 et al., 2006), and establishment of cell polarity during migration (Murawala et al., 2009).
50 Furthermore, heterotrimeric kinesin-2 is reported to play critical roles in mitosis (Fan et al., 2004;
51 Haraguchi et al., 2006).

52
53 Cilia assemble in quiescent cells and disassemble in dividing cells (Plotnikova et al., 2009).
54 In quiescent cells, heterotrimeric kinesin-2 is localized in both cilia and basal body in ciliated
55 cells. In dividing cells, when cells enter mitosis and cilia retract, the non-motor subunit KAP3 is
56 transported into nucleus before nuclear membrane break down in cells of sea urchin blastulae
57 (Morris et al., 2004). During cytokinesis, the motor protein KIF3B is localized in the midbody
58 (Fan et al., 2004). Macromolecules can't freely go into or out of the cilium and nucleus because
59 diffusion barriers exist at the ciliary base and the nuclear pore complex (NPC) (Kee et al., 2012;
60 Breslow et al., 2013; Takao et al. 2014., Endicott et al., 2018). The fundamental question is how
61 this conserved heterotrimeric kinesin-2 complex traffics between different compartments (the
62 cytoplasm, nucleus and cilium) for specific functions, and how these processes are regulated.

63
64 For nuclear transport from the cytoplasm, the NPC mediates active transport of proteins
65 (Alber et al., 2007; Wenthe SR et al., 2010; Strambio-De-Castillia et al., 2010; Beck et al., 2017).
66 Larger proteins (>50 kDa) generally require RanGTP and specific importin transport receptors to

67 cross the NPC (Gorlich et al., 1994; Gorlich and vogel et al., 1995). Importins usually bind a
68 nuclear localization signal (NLS)-containing cargo at relatively low RanGTP level in cytosol. This
69 moves the complex through NPCs and releases cargo in the nucleus where RanGTP
70 concentration is high (Moore et al., 1993; Gorlich et al., 1999). In most cases, importin β binds
71 to importin α , which interacts with a conventional NLS, to mediate substrate nuclear import
72 (Gorlich and Kostka et al., 1995). In contrast, importin β recognizes non-traditional proline-
73 tyrosine NLS (PY-NLS) for nuclear import (Lee et al., 2006). In the nucleus, direct binding of
74 RanGTP with importin β results in cargo release (Gorlich et al., 1997).

75
76 Compared to nucleo-cytoplasmic transport, the molecular mechanisms or sequence motifs
77 controlling membrane or soluble protein trafficking into cilia are less well understood. Previous
78 studies reported that several cis-acting elements, including RVxP, VxPx, and Ax[S/A]xQ motifs,
79 are important for mediating ciliary trafficking of membrane proteins (Jenkins et al., 2006; Geng
80 et al., 2006; Mazelova et al., 2009; Berbari et al., 2008). Several recent studies implicated that
81 the cilium and nucleus are co-evolved for signal integration because of the shared components
82 and evolutionary origin (McClure-Begley et al., 2017; Johnson et al., 2019; Satir et al., 2019). It
83 was also proposed that there are some shared mechanisms between ciliary import and nuclear
84 import (Dishinger et al., 2010; Takao et al., 2014; Del Viso et al., 2016; Takao et al., 2017;
85 Endicott et al., 2018). Several results indicated that RanGTP/importin β /NLS import system is
86 required for ciliary targeting of either membrane or soluble proteins including importin β 1 for
87 Crumbs3 (Fan et al., 2007), RanGTP/importin β 2 for KIF17 and Gli2 (Tarrado et al., 2016;
88 Dishinger et al., 2010), importin β 2 for RP2 (Hurd et al., 2011), importin α 1/ α 6/NLS for KIF17
89 (Funabashi et al., 2017), and importin β 2/PY-NLS for GLI2/GLI3 (Han et al., 2017). It was also
90 reported that importin β 2/Rab8 forms a ternary complex with ciliary localization sequences to
91 direct membrane protein trafficking to cilia (Madugula et al., 2016), suggesting that this process
92 is independent of RanGTP and a NLS or PY-NLS. Despite these advancements in uncovering
93 mechanisms for ciliary import, it remains unclear whether RanGTP regulates ciliary trafficking
94 directly or by affecting nuclear import to result in defective ciliary trafficking. It is also unclear
95 whether different cargoes depend on different importin β receptors for ciliary trafficking. Lastly,
96 prior work investigated determinants of ciliary entry for the homodimeric ciliary kinesin
97 composed of KIF17 (Dishinger et al., 2010), the heterotrimeric kinesin-2 is the motor that
98 dictates cilium assembly and maintenance (Walther et al., 1994; Morris et al., 1997; Sarpal et
99 al., 2004; Zhao et al., 2011; Engel et al., 2009; Ludington et al., 2013). Therefore, we focused
100 on how ciliary trafficking of the heterotrimeric kinesin-2 is regulated by leveraging the unique

101 advantages of the unicellular green alga *Chlamydomonas reinhardtii* as an excellent eukaryotic
102 model to study ciliogenesis (Harris et al., 2001; Rosenbaum et al., 2002).

103

104 Cilia of *Chlamydomonas* can be regenerated to full length in two hours, and unlike
105 mammalian cells, ciliary assembly does not need to be induced (Rosenbaum et al., 1969) to
106 result in heterogeneous population of ciliated and non-ciliated cells. The molecular mechanism
107 of the nucleo-cytoplasmic trafficking is likely conserved between the *Chlamydomonas* and
108 humans (Li et al., 2018). However, there are fewer constituent nucleoporins in the
109 *Chlamydomonas* NPC compared to that of humans (Neumann et al., 2006). By using both
110 mammalian and *Chlamydomonas* cells, we have found that ciliary trafficking of kinesin
111 associated protein KAP3 is regulated by RanGTP. We demonstrated that precise manipulation
112 of RanGTP level is crucial for regulating cilium formation. Importantly, we were able to clearly
113 show that RanGTP plays a direct role in incorporation of ciliary proteins that is independent of
114 its nuclear roles. These results provide potential insights for the molecular mechanism
115 orchestrating multi-compartment trafficking of the heterotrimeric kinesin-2 motor complex.
116 Further, they answer a long-standing open question in the field about whether nuclear import
117 mechanisms have been coopted for direct ciliary import.

118

119 **Results**

120 **Ciliary protein KAP3 can localize to the nucleus**

121 The heterotrimeric kinesin-2 motor complex consists of the heterodimeric motor proteins
122 KIF3A/3B and the adaptor protein KAP3. In contrast, the homodimeric kinesin-2 KIF17 motor
123 does not need an adaptor protein to exert its function. Although it was suggested that KAP3
124 functions as a linker between KIF3A/3B and the specific cargoes to facilitate intracellular
125 transport, the function of KAP3 is still not well characterized. To explore this, we firstly
126 investigated the intracellular localization of KAP3 in ciliated and non-ciliated cells. HA-tagged
127 KAP3A and KAP3B (a short isoform of KAP3A) were transfected into hTERT-RPE cells. 24
128 hours after transfection, cilia were induced by serum starvation. As expected, both HA-tagged
129 KAP3A and KAP3B co-localized with acetylated- α -tubulin, confirming the intracellular
130 localization of KAP3A and KAP3B are not affected by small HA epitope and can be targeted to
131 cilia (**Figure 1A**). Surprisingly, we noticed that a significant amount of KAP3A and KAP3B was
132 also distributed throughout the nucleus (**Figure 1A**). We further examined the localization of
133 KAP3A and KAP3B in other different cell types. As shown in **Figure 1B**, HA-tagged KAP3A and
134 KAP3B are mainly localized in the nucleus of COS-7 cells, although a small amount is

135 distributed in the cytoplasm. We also showed that EGFP-tagged KAP3A and KAP3B could
136 localize in the nucleus of MDCK cells (**Figure 1C**). Nuclear localization of KAP3A was
137 consistent with that of EGFP tagged KAP3A in a previous report (Tenny et al., 2016).

138 To dissect critical regions within KAP3A responsible for its nuclear localization, as depicted
139 in **Figure 1D**, EGFP-fused KAP3 truncations were constructed (henceforth, KAP3 refers to the
140 long isoform KAP3A). First, the expression of appropriately-sized truncations in MDCK cells was
141 detected by western blot analysis (**Figure 1E**). Second, the subcellular distributions of these
142 KAP3 truncations in MDCK cells were analyzed via fluorescence microscopy. As shown in
143 **Figure 1F**, the N-terminal fragment KAP3 (1-270) and the C-terminal fragment KAP3 (661-792)
144 are distributed in both the cytoplasm and nucleus, and KAP3 (271-460) was exclusively
145 distributed in the cytoplasm. In contrast, KAP3 (461-660), consisting of armadillo repeats (ARM)
146 6-9, were predominantly localized in the nucleus, which is similar to full-length KAP3. These
147 data indicate that the region between amino acids 461 and 660 is crucial for nuclear localization
148 of KAP3. Taken together, our data demonstrate that ciliary protein KAP3 can localize to the
149 nucleus under the control of armadillo repeats 6-9.

150

151 **RanGTP, but not importin β 2, mediates nuclear translocation of KAP3**

152 As shown in **Figure 1**, KAP3 is distributed to the nucleus in different cells. To determine the
153 molecular mechanism of KAP3 nuclear translocation, we tested a well-studied pathway for
154 protein nuclear import, RanGTP mediated nuclear import, which requires a high concentration of
155 RanGTP in the nucleus for the disassembly of the imported complexes. To determine whether
156 RanGTP drives nuclear import of KAP3, the dominant negative mutant RanQ69L which cannot
157 hydrolyze GTP, was used in this study. As shown in **Figure 2A**, Ectopic expression of RanQ69L
158 blocked nuclear localization of KAP3 in COS-7 cells, resulting in a more cytoplasmic distribution
159 of KAP3 relative to wild-type controls. This data suggests that nuclear translocation of KAP3 is
160 mediated by a RanGTP-dependent nuclear import pathway.

161 We mapped the region responsible for nuclear localization of KAP3 and found that KAP3
162 (461-660) is required. If the region we mapped is correct, the nuclear localization of this
163 truncation KAP3 (461-660) should be RanGTP-dependent, which act the same way as full-
164 length KAP3. To test this, we co-transfected KAP3 (461-660) with the dominant negative Ran
165 mutant RanQ69L. As shown in **Figure 2B**, RanQ69L completely disrupted nuclear import of
166 KAP3 (461-660) and resulted in the cytoplasmic localization of this truncation. These results
167 suggest that RanGTP-dependent nuclear import of KAP3 is dependent on the 461-660 region of

168 KAP3. In contrast, RanQ69L didn't change the localization of other KAP3 truncations (**Figure**
169 **2B**).

170 It was reported that the import receptor importin β 2 plays critical roles in both nuclear import
171 and ciliary import of ciliary proteins, like KIF17 and GLI2/GLI3 (Dishinger et al., 2010; Han et al.,
172 2017). We further examined whether importin β 2 is utilized for nuclear translocation of KAP3.
173 The importin β 2 inhibitory peptide M9M was used in these studies (Cansizoglu et al., 2007).
174 hnRNP A1 was used as a positive control for this assay. As shown in **Figure S1A**, expression of
175 MBP-tagged M9M inhibitory peptide disrupted nuclear localization of hnRNPA1 (*white arrow*),
176 which confirmed that hnRNP A1 utilizes transport receptor importin β 2 for its nuclear
177 translocation. Compared to the empty MBP control, MBP-tagged M9M did not block the nuclear
178 translocation of KAP3 (**Figure S1B**). This data suggests nuclear import of KAP3 is independent
179 of the importin β 2 receptor.

180

181 **The armadillo repeat domain 6-9 (ARM6-9) alone is sufficient for ciliary base localization.**

182 KAP3 can localize in both the cilium and nucleus. We dissected the regions required for
183 nuclear translocation of KAP3. Next, we mapped the regions required for ciliary targeting of
184 KAP3 in hTERT-RPE cells. As depicted in **Figure 3A**, full-length KAP3 contains three regions: a
185 non-conserved N-terminal domain, nine armadillo repeats, and a C-terminal conserved domain
186 (Jimbo et al., 2002; Shimuzu et al., 1996). Based on this, a series of truncations of KAP3 were
187 generated and intracellular localization of these truncations was examined after cilium induction.
188 As shown in **Figure 3B**, the truncation KAP3 (661-792) containing the C-terminal domain
189 completely abolished localization to the cilium and ciliary base. In contrast, the truncation
190 KAP3(186-792) containing both the nine armadillo repeats and C-terminal domain, and the
191 truncation KAP3(186-660) merely with the nine armadillo repeats showed intense signal at the
192 ciliary base. These data suggest that the nine armadillo repeats are required for KAP3 targeting
193 to the ciliary base. We further narrowed the region within the nine armadillo repeats and
194 demonstrated that the truncation KAP3(461-660), harboring the ARM6-9, is sufficient for ciliary
195 base targeting of KAP3 (**Figure 3B**). It is noteworthy that this region is also required for
196 RanGTP mediated KAP3 nuclear trafficking.

197

198 **RanGTP regulates percent ciliation in human retinal epithelial cells**

199 Given the middle region of KAP3, 461-660, is required for both nuclear and cilium base
200 targeting and nuclear targeting is RanGTP dependent, we wanted to investigate whether KAP3-
201 dependent ciliogenesis and cilium length regulation (Sarpal et al., 2003; Mueller et al., 2004),

202 was also RanGTP dependent. We were further interested in Ran-dependent ciliary phenotypes
203 and KAP3 localization due to previously reported shared mechanisms between nuclear and
204 ciliary import processes (Dishinger et al., 2010; Takao et al., 2014; Del Viso et al., 2016; Takao
205 et al., 2017; Endicott et al., 2018) and conflicting conclusions about the effect of RanGTP on
206 ciliogenesis (Dishinger et al., 2010; Fan et al., 2011; Torrado et al., 2016). Wild-type Ran and
207 three well-characterized dominant negative Ran mutants (RanQ69L, RanG19V and RanT24N)
208 were used in this study. First, we studied the intracellular localization of these proteins in
209 hTERT-RPE cells in serum-starved condition which induce ciliogenesis. As shown in **Figure S2**,
210 all the mutants are predominantly localized in the nucleus which is similar to that of wild-type
211 Ran. These data indicate that expression of these point mutants did not dramatically affect
212 intracellular localization of Ran. To analyze the role of these mutants in cilium formation and
213 length regulation in hTERT-RPE cells, wild type and mutant Ran expression plasmids were
214 transfected into hTERT-RPE cells. 24 hours post-transfection, low serum media were added for
215 24 hours to induce cilium formation. As shown in **Figure 4A and 4C**, ectopic expression of
216 either the GTP locked mutants RanQ69L/RanG19V or the GDP-locked mutant RanT24N had no
217 obvious effect on cilium length. In contrast, cells transfected with these dominant negative
218 mutants could reduce ciliation percentage compared the un-transfected control cells (**Figure**
219 **4B**). Further, different Ran mutants had different effects on ciliation percentage. RanQ69L has
220 higher affinity to GTP and resulted in a dramatically reduction in ciliation percentage compared
221 to RanG19V, which has relatively low affinity to GTP (Lounsbury et al., 1996) (**Figure 4B**).
222 These data indicate that the RanGTP level in hTERT-RPE cells is a determinant of initiation of
223 cilium formation. Taken together, the ability to bind and hydrolyze GTP by Ran in vivo, revealed
224 by different dominant Ran mutants, regulates its essential functions on the generation of cilia.

225 To determine why there is reduced cilium formation in RanQ69L-expressing RPE cells, we
226 further investigated the localization of other important components, like the IFT complex and
227 kinesin-2. As shown in **Figure 4D**, IFT81, a component of the IFT-B complex, is still localized in
228 the ciliary base of hTERT-RPE cells expressing RanQ69L, suggesting that IFT-B targeting is not
229 affected and is unlikely to be the primary cause of defective cilium formation. In contrast, the
230 kinesin-2 associated protein KAP3 didn't localize to the ciliary base. This data suggests that, in
231 addition to potential roles for RanGTP in ciliary entry, ciliary targeting of the heterotrimeric
232 kinesin-2 is also RanGTP-dependent.

233

234 **RanGTP regulates ciliary length and ciliary trafficking of KAP under steady-state**
235 **conditions in *Chlamydomonas***

236 To see if mechanisms of Ran-dependent ciliary targeting and entry are broadly conserved,
237 we tested the effect of Ran manipulation on assembly and kinesin-2 motor targeting in
238 *Chlamydomonas* cilia. The unicellular green algae *Chlamydomonas* is an excellent model to
239 study ciliary length regulation and protein trafficking. In addition to the extensive body of
240 literature on motor trafficking and ciliary assembly in this organism, the small G-protein Ran and
241 key residues required for GTP hydrolysis are well conserved between humans and
242 *Chlamydomonas* (**Figure S3**). We therefore examined the role of Ran-like protein (Ran1), the
243 ortholog of human Ran, on ciliary length regulation in wild-type *Chlamydomonas* CC-125 cells.
244 Importazole (IPZ), a small molecular inhibitor which specifically blocks RanGTP-importin β 1
245 interaction (Soderholm et al., 2011), was used to perturb RanGTP function. The result indicated
246 treatment CC-125 cells with IPZ for 2 hours shortens ciliary length in a dose-dependent manner
247 (**Figure 5, A and B**).

248 To exclude that the phenotype was caused by the off-target effect of the inhibitor, the GTP-
249 locked Ran1 mutant Ran1Q73L, corresponding to human RanQ69L, was transformed into
250 *Chlamydomonas*. As shown in **Figure 5C**, there is strong Ran1Q73L expression as expected in
251 *Chlamydomonas* (green arrow), despite a portion of expressed Ble-2A-Ran1Q73L fusion
252 proteins being incompletely processed due to the cleavage efficiency of 2A peptide in
253 *Chlamydomonas* (red arrow). Compared to control cells with normal ciliary length and cell
254 division, the cells expressing high levels of Ran1Q73L exhibits either clumpy cells or shortened
255 ciliary length. One possible explanation for clumpy cells may be that there are no cilia to secrete
256 ectosomes containing lytic enzyme to break the cell wall after cell division (Wood et al., 2013).
257 These results demonstrated that RanGTP plays pivotal roles in ciliary length regulation in
258 *Chlamydomonas*.

259 We showed that KAP3, but not IFT81, couldn't be targeted to ciliary base in hTERT-RPE
260 cells constitutively expressing GTP-locked RanQ69L. It was reported that RanGTP regulates
261 ciliary entry of the other motor KIF17, which is localized in the nucleus as KAP3 (Dishinger et
262 al., 2010). Based on these data, we tested whether perturbing Ran function affected ciliary
263 targeting or entry of KAP, the ortholog of human KAP3, in the *Chlamydomonas* KAP-GFP
264 reporter strain CC-4296. As shown in **Figure 5D**, KAP-GFP is distributed in both the cilium and
265 cilium base in control cells treated with DMSO. In contrast, ciliary localization of KAP-GFP was
266 dramatically decreased in the cells treated with 20 μ M IPZ for 2 hours. These results indicate
267 that ciliary localization of KAP is regulated by RanGTP in *Chlamydomonas*. To further
268 investigate whether IPZ directly affects ciliary entry of KAP, we used real-time total internal
269 reflection fluorescence microscopy (TIRFM) to study the dynamic behavior of KAP. Kymograph

270 analysis showed that KAP could enter into the cilium in un-treated cells. In contrast, ciliary entry
271 of KAP is blocked in the cells treated with 50 μ M IPZ (**Figure 5E**). The image shown was taken
272 around 20 minutes after addition of IPZ indicating a direct role of RanGTP in regulation of ciliary
273 entry of the motor subunit KAP as propagation of nuclear effects are likely to take longer than
274 the immediate reduction in ciliary entry upon drug addition.

275

276 **RanGTP directly regulates ciliary protein incorporation during cilia regeneration in** 277 ***Chlamydomonas***

278 One advantage of the *Chlamydomonas* model system in this context is the significant
279 available information about requirements for nuclear regulation of ciliary assembly. During ciliary
280 regeneration after ciliary severing (deciliation), new ciliary proteins need to be synthesized and
281 transported to assembly sites for incorporation into cilia (**Figure 6A**). This process requires
282 initiating gene expression, which would be dependent on nuclear import of specific transcription
283 factors like XAP5 (Li et al., 2018). Therefore, it is possible that RanGTP regulates cilium length
284 by indirectly affecting nuclear import and ultimately new transcription/ciliary protein synthesis.
285 To tease apart nuclear and non-nuclear effects, we were able to use the small molecular
286 inhibitor cycloheximide (CHX) to inhibit new protein synthesis during cilia regeneration. As
287 shown in Figure 6A, in wild-type *Chlamydomonas* cells, this typically results in growth of cilia to
288 half-length (6 μ m) which exhibits the ability of these cells to incorporate already-synthesized
289 proteins to generate half-length cilia without the production of new proteins from the burst of
290 transcription post-deciliation (Rosenbaum et al., 1969). As expected, when blocking new protein
291 synthesis with CHX, the existing ciliary proteins can build short cilia as shown in **Figure 6B**. If
292 RanGTP exclusively inhibits nuclear import, but not ciliary import, inhibition of Ran function
293 should allow existing ciliary proteins to still incorporate and assemble cilia to half-length (**Figure**
294 **6A, Model 1**). If inhibiting Ran function blocks both nuclear import and direct ciliary import, even
295 the existing ciliary proteins shouldn't incorporate and build cilia, resulting in bald cells (**Figure**
296 **6A, Model 2**). Our data fit Model 2 and show that when the deciliated cells are treated with IPZ
297 to inhibit Ran function (with CHX to block any new protein synthesis), there is no cilium
298 formation during regeneration. This demonstrates that IPZ can directly block incorporation of the
299 existing ciliary proteins into cilia for assembly (**Figure 6B**). To confirm that the lack of ciliary
300 growth wasn't due to cell toxicity and that IPZ only impacts the ability of existing proteins to
301 enter cilia, we washed out IPZ but still continued CHX treatment to inhibit new protein synthesis.
302 As shown in **Figure 6 C and D**, ciliary biogenesis is restored upon IPZ washout. These data
303 clearly showed that under conditions where only existing ciliary proteins can either enter cilia or

304 not, RanGTP has direct effects in regulating ciliary protein incorporation. We also released CHX
305 inhibition to confirm that, regardless of the presence of new proteins, blocking Ran function can
306 regulate incorporation of existing ciliary proteins expected to enter cilia upon deciliation (**Figure**
307 **S4 A and B**). Our data indicated IPZ can block incorporation of the existing ciliary proteins in
308 addition to any newly synthesized proteins. In these conditions, if IPZ blocked nuclear entry of
309 transcription factors needed for the spike in ciliary proteins but did not directly affect ciliary entry
310 of existing proteins, cilia would still reach half-length from the already-synthesized ciliary protein
311 pool. Ultimately, given the dual role of RanGTP in mediating ciliary import and nuclear import, it
312 is important to segregate nuclear and direct ciliary effects of Ran perturbation. Here we are able
313 to show that in spite of its demonstrated roles in regulating nuclear protein import, RanGTP has
314 direct roles in mediating ciliary protein incorporation for cilia formation.

315

316 **Discussion**

317 Although most kinesin motors are localized in the cytoplasm, different conditions allow
318 some kinesin motors to transport into the nucleus including KAP3, KIF4, KIF17, and KIF17B
319 (Morris et al., 2004; Seungoh et al., 2001; Dishinger et al., 2010; Macho et al., 2002). KAP3 and
320 KIF4 can redistribute to the nucleus during mitosis (Morris et al., 2004; Seungoh et al., 2001).
321 During mouse spermatid development, KIF17B shuttles from nucleus to cytoplasm (Macho et
322 al., 2002). We observed that both the isoforms of the heterotrimeric kinesin-2 accessory subunit
323 KAP3A and KAP3B are localized in the nucleus, and that their nuclear localization is RanGTP
324 dependent. Considering KIF17B can function as a transcription regulator (Macho et al., 2002), it
325 is possible that KAP3 participates in regulation of gene expression in the nucleus. Besides the
326 kinesin motors, many cilia associate proteins can localize in the nucleus (McClure-Begley et al.,
327 2017). The exchange of components between the ciliary and nuclear compartments is also
328 thought to be mediated by membrane-less organelles (Johnson et al., 2019). However, the
329 nuclear roles and origin of cilia associated proteins needs to be further investigated.

330 It was reported that the armadillo repeats of KAP3 are responsible for binding to motor
331 subunits KIF3A/3B, and the C-terminal conserved domain is responsible for specific cargo
332 binding (Haraguci et al., 2005; Nagata et al., 1998; Jimbo et al., 2002; Deacon et al, 2003). Our
333 data showed the armadillo repeats 6-9 (ARM6-9) is required for KAP3 targeting to the ciliary
334 base, probably mediated by RanGTP. It is possible that the heterodimeric KIF3A/3B and
335 RanGTP collaboratively regulate KAP3 targeting to the ciliary base. It is also noteworthy that
336 cells expressing the truncated KAP3A (186-660), containing only the armadillo repeat domain,
337 have normal cilia length, whereas cells expressing the truncated KAP3 (186-792), containing

338 both the armadillo repeats and cargo-binding domains, have no cilia. Given that loss of the
339 cargo-binding domain dramatically decreases KAP3 binding to KIF3A/3B (Haraguci et al.,
340 2005), our data suggest that the dominant negative function of KAP3 truncations is dependent
341 upon their binding ability to the KIF3A/KIF3B motor subunits.

342 Several lines of evidence suggest that RanGTP is involved in ciliary protein trafficking
343 (Dishinger et al., 2010; Hurd et al., 2001; Fan et al., 2011; Maiuri et al., 2013). RanGTP was
344 reported to regulate ciliary entry of the homodimeric motor KIF17 and RP2 (Dishinger et al.,
345 2010; Hurd et al., 2001). RanGTP was also reported to facilitate ciliary export of huntingtin
346 (Maiuri et al., 2013). However, there role of RanGTP on cilium formation was ambiguous. Two
347 groups demonstrated that RanGTP has no effect on ciliary biogenesis (Dishinger et al., 2010;
348 Torrado et al., 2016), whereas another group showed that manipulation of RanGTP
349 concentration via RanBP1 knockdown could drive cilia formation (Fan et al., 2011). The
350 difference of these observations for the role of RanGTP on cilia formation may be due to
351 different cell lines, different strategies for inhibiting RanGTP function, or the timing and levels of
352 RanGTP inhibition relative to cilia induction. Our results indicate that different dominant negative
353 forms of Ran have different effects on cilia formation, although these mutants have no effect on
354 regulating cilium length. Furthermore, GTP locked mutant RanQ69L more dramatically affects
355 percent ciliation than that of RanG19V. The difference between RanQ69L and RanG19V is that
356 RanQ69L has much higher affinity for GTP than RanG19V, thus RanQ69L-expressing cells
357 have less free RanGTP than RanG19V-expressing cells. Taken together, our results suggest
358 that precise manipulation of intracellular free RanGTP is critical for regulating cilium formation.

359 In addition to RanGTP, the importin transport receptors also participate in ciliary protein
360 trafficking (Fan et al., 2007; Dishinger et al., 2010; Hurd et al., 2001; Torrado et al., 2016;
361 Madugula et al., 2016; Han et al., 2017). There is also some disagreement about which importin
362 is utilized for ciliary protein trafficking. Importin β 1 was responsible for transmembrane protein
363 Crumbs3 ciliary trafficking (Fan et al., 2007), and importin β 2 was identified as the transport
364 receptor for ciliary targeting of either transmembrane or soluble proteins like KIF17, Gli2 and
365 Gli3 (Dishinger et al., 2010; Hurd et al., 2001; Madugula et al., 2016; Torrado et al., 2016; Han
366 et al., 2017). However, additional data has shown that importin α 1 and α 6, but not importin β 2,
367 are responsible for ciliary targeting of soluble KIF17 (Funabashi et al., 2017). In general,
368 importin β 1, alone or in cooperation with importin α , transports substrates with a conventional
369 NLS (Lange et al., 2007), whereas importin β 2 transports substrates that contain the non-
370 conventional PY-NLS (Lee et al., 2006). Consistent with this, ciliary targeting of the
371 transcriptional factor Gli2/Gli3, which utilizes transport receptor importin β 2, relies on its PY-NLS

372 motif. PY-NLS mutations also result in the loss of Gli2/Gli3 ciliary targeting (Han et al., 2017). It
373 is reported that the NLS-like sequence in the C-terminal region of KIF17 is required for its ciliary
374 targeting (Dishinger et al., 2010). This NLS-like sequence was further confirmed as a classical
375 mono-partite NLS (Funabashi et al., 2017). However, we noticed that PL, the PY variant, is
376 located in the immediate downstream region of this NLS. So it is worth investigating whether or
377 not this C-terminal NLS of KIF17 is a PY-NLS and which importin is used for KIF17 ciliary
378 trafficking. Recently, a ternary complex consisting of importin β 2, small GTPase Rab8 and
379 ciliary targeting signals was reported to guide transmembrane protein trafficking to cilium
380 (Madugula et al., 2016). This data suggests that spatial structure of the ternary complex, but not
381 specific ciliary targeting sequences, are required for ciliary targeting of membrane proteins. This
382 highlights that the detailed working model for how importin mediates ciliary import needs to be
383 further clarified.

384 There is increasing data that nuclear import and ciliary import shares similar mechanisms,
385 at least in part (Dishinger et al., 2010; Kee et al., 2012; Takao et al., 2014; Del Viso et al., 2016;
386 Takao et al., 2017; Endicott et al., 2018). First, both the NPC and the ciliary pore complex form
387 a diffusion barrier (Kee et al., 2012; Endicott et al., 2018). Second, the RanGTP/importin
388 transport system is also used for ciliary protein trafficking (Fan et al., 2007; Dishinger et al.,
389 2010; Hurd et al., 2011; Han et al., 2017). Third, some nucleoporins also localize in the ciliary
390 base to regulate barrier diffusion ability (Dishinger et al., 2010; Del Viso et al., 2016; Endicott et
391 al., 2018). Our data have shown that RanGTP can regulate cilium formation and ciliary
392 trafficking of KAP3. One remaining critical question is whether RanGTP has direct effects in
393 modulating ciliary protein transport. One possibility is that the effect of RanGTP is an indirect
394 result of inhibiting nuclear import of proteins, like transcriptional factors, which are required for
395 ciliary formation. By using the unicellular green alga *Chlamydomonas* as a model organism, we
396 clearly demonstrated that RanGTP function directly regulates ciliary incorporation of the existing
397 pool of already-synthesized ciliary proteins, which is not dependent on new transcription. In
398 addition, the dominant negative mutant RanQ69L blocked ciliary trafficking of KAP3. Given that
399 KAP is required for localization of KIF3A/3B to the assembly sites (Muller et al., 2005), RanGTP
400 may control cilia formation by directly regulating ciliary targeting of the heterotrimeric kinesin-2
401 motor. This will in turn affect ciliary assembly and length maintenance due to the importance of
402 ciliary recruitment and entry of kinesin-2 motor KIF3A/3B/KAP in these processes (Engel et al.,
403 2009; Ludington et al., 2013). Further work will determine if this is a generalized mechanism for
404 ciliary protein import and will identify additional RanGTP-regulated ciliary proteins (cargoes)
405 required for cilium assembly, length control, and function.

406

407 **Materials and Methods**

408 **Compounds**

409 DMSO, Importazole (IPZ, #SML0341) and Cycloheximide (C1988) were purchased from Sigma-
410 Aldrich. Indicated concentrations and specific incubation times are used in this study.

411

412 **DNA constructs**

413 Plasmids for HA-tagged human KAP3A and KAP3B were kindly from Dr. Benjamin Allen
414 (University of Michigan). Plasmids for wild-type Ran and point mutants RanG19V and RanT24N
415 are a generous gift from Dr. Kristen Verhey (University of Michigan). Plasmids expressing MBP
416 and M9M were from Dr. Yuh Min Chook (University of Texas Southwestern Medical Center).
417 Plasmids pmCherry-C1-RanQ69L (#30309) was obtained from Addgene under the material
418 transfer agreement. GeneArt™ *Chlamydomonas* protein expression vector pChlamy_4 was from
419 Thermo Fisher Scientific. Recombinant plasmids pChlamy_4_Ran1Q73L, EGFP or HA-tagged
420 KAP3 truncations were generated by ligation-independent cloning strategy as described before
421 (Zhu et al., 2010) and sequenced in full.

422

423 ***Chlamydomonas* strains, mammalian cells and antibodies**

424 Wild-type and KAP-GFP reporter strains were obtained from the *Chlamydomonas* resource
425 center (CC-125 mt⁺ and CC-4296). Strains were grown in liquid Tris-Acetate-Phosphate (TAP)
426 liquid medium for 18-24 hours prior to experimentation. Mammalian COS-7 and MDCK Cells
427 were cultured in Dulbecco's Modified Eagle's Medium (DMEM; Invitrogen) supplemented with
428 10% fetal bovine serum (FBS; Invitrogen). Human TERT-RPE cells were cultured in
429 DMEM+F12 (1:1) (Invitrogen) containing 10% FBS. Antibodies used in this study are as follows
430 (IF and WB are short for immunofluorescence and western blot, respectively): Mouse anti-
431 acetylated α -tubulin (#T6793, 1:500 for IF) was from Sigma-Aldrich (St. Louis, MO, USA).
432 Rabbit anti-Cep164 (#22227-1-AP, 1:50 for IF) and rabbit anti-IFT81 (#11744-1-AP, 1:50 for IF)
433 were from Proteintech. Mouse anti-KAP3A (#610637, 1:20 for IF) was from BD Transduction
434 Laboratories™. Mouse anti-Myc (AB_390912, 1:100 for IF) was from Roche. Mouse anti-hnRNP
435 A1 Antibody (sc-32301, 1:50 for IF) was from Santa Cruz biotechnology. Rabbit anti-myc
436 (#5625, 1:500 for IF), Rabbit anti-V5 (#13202, 1:1000 for WB), rabbit anti-HA (#3724, 1:100 for
437 IF) and Rabbit anti-GFP (#2956, 1:100 for IF and 1:1000 for WB, respectively) were from Cell
438 Signaling Technology.

439

440 **Cell culture and transfection**

441 COS-7, MDCK and hTERT-RPE cells were maintained in a humidified atmosphere at 37°C and
442 5% CO₂. Cells for transfection were seeded in an 8-well chamber slide (Lab-Tek) with 0.4 mL
443 culture medium per well. After overnight growth, the cells became 70-80% confluent and were
444 transfected with the corresponding plasmids using the transfection reagent FuGENE 6 (Roche)
445 according to the manufacturer's instructions. In normal condition, COS-7, MDCK and hTERT-
446 RPE cells are fixed with 4% paraformaldehyde for intracellular localization assay 24 hours post-
447 transfection. In serum starvation condition for cilium induction, hTERT-RPE cells were cultured
448 in complete medium for 24 hours post-transfection, then followed to culture in DMEM+F12 (1:1)
449 with 0.25% FBS for other 24 hours.

450

451 ***Chlamydomonas* transformation**

452 Electroporation transformation was used form rapid transformation of *Chlamydomonas* with the
453 electroporator NEPA (Nepa Gene, Japan). Transformation was performed following the
454 published protocol with some modifications (Yamano et al., 2013). The typical 4 days were
455 necessary to perform the transformation. *Day 1*: pre-cultivation stage: the cells were grown in 5
456 mL TAP liquid medium for overnight culture. *Day 2*: pre-cultured cells from day 1 were
457 transferred into a new 50 mL TAP medium in a 250 mL flask with a final OD₇₃₀ of 0.1 (usually 1-3
458 mL pre-cultures added) for overnight culture with 120 rpm/25°C. *Day 3*: cells were harvested by
459 centrifugation when the cell density reached OD₇₃₀ of 0.3-0.4, and washed by GeneArt MAX
460 Efficiency Transformation Reagent (Invitrogen) 3 times and re-suspended in 250 µL TAP
461 medium containing 40 mM sucrose. 1.6 µg linearized DNA (pChImay_4_Ran1Q73L) was mixed
462 with 160 µL of the cell suspension for electroporation. After electroporation, the cells were
463 transferred into 10 mL TAP plus 40 mM sucrose for overnight culture in dim light. *Day 4*: cells
464 were collected and plated onto 1.5% TAP-agar plate with 10 µg/mL zeocin for growth. The
465 colonies will be visible 5-7 days later.

466

467 **Immunofluorescence staining**

468 Cells were washed with cold PBS twice, and then fixed with 4% paraformaldehyde in HEPES
469 (pH 7.4) for 15 min at room temperature. Cells were washed three times with cold PBS and then
470 incubated with 0.1% Triton X-100 in PBS (pH 7.4) for 10 min. Permeabilized cells were washed
471 with PBS three times, and then incubated in PBS with 10% normal goat serum and 1% BSA for
472 1 hour at room temperature to block non-specific binding of the antibodies. Cells are incubated
473 with diluted primary antibody in PBS with 1% BSA overnight at 4°C. After three times wash with

474 PBS, cells are incubated with the secondary antibody in PBS with 1% BSA for 1 hour at room
475 temperature in the dark. After washing three times with PBS, cells are mounted with ProLong
476 Antifade mounting medium with or without DAPI, and kept at 4°C in the dark for further imaging.

477

478 **TIRF Microscopy**

479 Samples were prepared as follows: KAP-GFP reporter cells (CC-4296) were cultured in TAP
480 liquid medium for 18 h, then centrifuged at 1000 rpm for 2 min. 3 µL cell pellets were re-
481 suspended in 200 µL TAP liquid medium containing either DMSO or 50 µM IPZ. 24 × 50 mm no.
482 1.5 coverslip was treated with 0.1% poly-lysine for 10 min, and dipped into water and let it air-
483 dry. Petroleum jelly was used to draw a circle around poly-lysine coated region. 20 µL of cells
484 were placed inside and allowed to settle for 3 min, and then imaged. KAP-GFP cells were
485 imaged on a Nikon Ti-E microscope with a 100x 1.49 NA oil objective. Images were obtained
486 at 23.95 fps with 0.16 µm per pixel by using an Andor DU897 electron multiplying charge-
487 coupled device (EMCCD) camera. The NIS-Elements software was used to crop the movies
488 and generate kymographs.

489

490 **Ciliary regeneration**

491 *Chlamydomonas* cells were deciliated by pH shock as described before (Witman et al., 1972),
492 and ciliary regeneration was induced in normal TAP liquid medium. After deciliation, cells were
493 immediately treated with 10 µg/mL Cycloheximide and/or 10 µM IPZ for 60 min. For IPZ
494 washout experiment, treated cells were washed 3 times and cultured in fresh TAP liquid
495 medium (or with 10 µg/mL Cycloheximide). Cells were fixed with 1% glutaraldehyde for 15 min
496 at room temperature, and cilia length was measured using the line segment tool in ImageJ.

497

498 **Statistical analyses**

499 All data are reported as mean values ± standard error of the mean (S.E.M). Graphs and
500 associated statistical analyses were performed with Prism 6.0C (GraphPad Software, La Jolla,
501 CA). The unpaired student's t-test was used to assess statistical significance of two groups. A
502 value of $p < 0.05$ was considered statistically significant.

503

504 **Competing interests**

505 The authors declare no competing or financial interests

506

507 **Acknowledgements**

508 We would like to thank Dr. Yuh Min Chook (University of Texas Southwestern Medical Center),
509 Drs. Kristen Verhey and Benjamin Allen (University of Michigan) for providing DNA plasmids.
510 We also thank our colleague Dr. Pamela Tran for sharing some reagents. We are grateful to the
511 members of Dr. Avasthi Lab for comments on the manuscript and Dr. Pawel Niewiadomski
512 (University of Warsaw) for feedback on our preprint. We would like to thank Ms. Larissa
513 Dougherty for editing the manuscript. This work was supported by the following grants: startup
514 of Department of Ophthalmology (P.A.) and the Biomedical Research Training Program (S.H.),
515 University of Kansas Medical Center; a postdoctoral fellowship from a Kansas Institutional
516 Development Award (IDeA) from the National Institute of General Medical Sciences of the
517 National Institutes of Health under grant number P20 GM103418 (S.H.).
518

519 **References**

- 520
521 Alber F, Dokudovskaya S, Veenhoff LM, Zhang W, Kipper J, Devos D, Suprpto A, Karni-Schmidt
522 O, Williams R, Chait BT, Sali A. The molecular architecture of the nuclear pore complex. *Nature*.
523 2007 Nov;450(7170):695
524
525 Anvarian Z, Mykytyn K, Mukhopadhyay S, Pedersen LB, Christensen ST. Cellular signalling by
526 primary cilia in development, organ function and disease. *Nature Reviews Nephrology*. 2019
527 Feb 7:1.
528
529 Beck M, Hurt E. The nuclear pore complex: understanding its function through structural insight.
530 *Nature reviews Molecular cell biology*. 2017 Feb;18(2):73
531
532 Berbari NF, Johnson AD, Lewis JS, Askwith CC, Mykytyn K. Identification of ciliary localization
533 sequences within the third intracellular loop of G protein-coupled receptors. *Molecular biology of*
534 *the cell*. 2008 Apr;19(4):1540-7
535
536 Breslow DK, Koslover EF, Seydel F, Spakowitz AJ, Nachury MV. An in vitro assay for entry into
537 cilia reveals unique properties of the soluble diffusion barrier. *J Cell Biol*. 2013 Oct
538 14;203(1):129-47.
539
540 Breslow DK, Holland AJ. Mechanism and regulation of centriole and cilium biogenesis. *Annual*
541 *review of biochemistry*. 2019 Jun 20
542
543 Cole DG, Diener DR, Himelblau AL, Beech PL, Fuster JC, Rosenbaum JL. Chlamydomonas
544 kinesin-II-dependent intraflagellar transport (IFT): IFT particles contain proteins required for
545 ciliary assembly in *Caenorhabditis elegans* sensory neurons. *The Journal of cell biology*. 1998
546 May 18;141(4):993-1008
547
548 Deacon SW, Serpinskaya AS, Vaughan PS, Fanarraga ML, Vernos I, Vaughan KT, Gelfand VI.
549 Dynactin is required for bidirectional organelle transport. *J Cell Biol*. 2003 Feb 3;160(3):297-301
550
551 Del Viso F, Huang F, Myers J, Chalfant M, Zhang Y, Reza N, Bewersdorf J, Lusk CP, Khokha
552 MK. Congenital heart disease genetics uncovers context-dependent organization and function of
553 nucleoporins at cilia. *Developmental cell*. 2016 Sep 12;38(5):478-92

554
555 Dishinger JF, Kee HL, Jenkins PM, Fan S, Hurd TW, Hammond JW, Truong YN, Margolis B,
556 Martens JR, Verhey KJ. Ciliary entry of the kinesin-2 motor KIF17 is regulated by importin- β 2 and
557 RanGTP. *Nature cell biology*. 2010 Jul;12(7):703
558
559 Endicott SJ, Brueckner M. NUP98 Sets the Size-Exclusion Diffusion Limit through the Ciliary Base.
560 *Current Biology*. 2018 May 21;28(10):1643-5
561
562 Engel BD, Ludington WB, Marshall WF. Intraflagellar transport particle size scales inversely with
563 flagellar length: revisiting the balance-point length control model. *The Journal of cell biology*.
564 2009 Oct 5;187(1):81-9
565
566 Fan J, Beck KA. A role for the spectrin superfamily member Syne-1 and kinesin II in cytokinesis.
567 *Journal of cell science*. 2004 Feb 1;117(4):619-29.
568
569 Fan S, Fogg V, Wang Q, Chen XW, Liu CJ, Margolis B. A novel Crumbs3 isoform regulates cell
570 division and ciliogenesis via importin β interactions. *The Journal of cell biology*. 2007 Jul
571 30;178(3):387-98.
572
573 Fan S, Whiteman EL, Hurd TW, McIntyre JC, Dishinger JF, Liu CJ, Martens JR, Verhey KJ,
574 Sajjan U, Margolis B. Induction of Ran GTP drives ciliogenesis. *Molecular biology of the cell*.
575 2011 Dec 1;22(23):4539-48.
576
577 Fliegauf M, Benzing T, Omran H. When cilia go bad: cilia defects and ciliopathies. *Nature reviews*
578 *Molecular cell biology*. 2007 Nov;8(11):880.
579
580 Funabashi T, Katoh Y, Michisaka S, Terada M, Sugawa M, Nakayama K. Ciliary entry of KIF17
581 is dependent on its binding to the IFT-B complex via IFT46–IFT56 as well as on its nuclear
582 localization signal. *Molecular biology of the cell*. 2017 Mar 1;28(5):624-33
583
584 Geng L, Okuhara D, Yu Z, Tian X, Cai Y, Shibasaki S, Somlo S. Polycystin-2 traffics to cilia
585 independently of polycystin-1 by using an N-terminal RVxP motif. *J Cell Sci*. 2006 Apr
586 1;119(7):1383-95
587
588 Görlich D, Kostka S, Kraft R, Dingwall C, Laskey RA, Hartmann E, Prehn S. Two different subunits
589 of importin cooperate to recognize nuclear localization signals and bind them to the nuclear
590 envelope. *Current Biology*. 1995 Apr 1;5(4):383-92
591
592 Görlich D, Kutay U. Transport between the cell nucleus and the cytoplasm. *Annual review of cell*
593 *and developmental biology*. 1999 Nov;15(1):607-60.
594
595 Görlich D, Prehn S, Laskey RA, Hartmann E. Isolation of a protein that is essential for the first
596 step of nuclear protein import. *Cell*. 1994 Dec 2;79(5):767-78
597
598 Görlich D, Vogel F, Mills AD, Hartmann E, Laskey RA. Distinct functions for the two importin
599 subunits in nuclear protein import. *Nature*. 1995 Sep;377(6546):246
600
601 Han Y, Xiong Y, Shi X, Wu J, Zhao Y, Jiang J. Regulation of Gli ciliary localization and Hedgehog
602 signaling by the PY-NLS/karyopherin- β 2 nuclear import system. *PLoS biology*. 2017 Aug
603 4;15(8):e2002063
604

- 605 Haraguchi K, Hayashi T, Jimbo T, Yamamoto T, Akiyama T. Role of the kinesin-2 family protein,
606 KIF3, during mitosis. *Journal of Biological Chemistry*. 2006 Feb 17;281(7):4094-9
607
- 608 Harris EH. *Chlamydomonas* as a model organism. *Annual review of plant biology*. 2001
609 Jun;52(1):363-406.
610
- 611 Hirokawa N, Noda Y, Tanaka Y, Niwa S. Kinesin superfamily motor proteins and intracellular
612 transport. *Nature reviews Molecular cell biology*. 2009 Oct;10(10):682
613
- 614 Hurd TW, Fan S, Margolis BL. Localization of retinitis pigmentosa 2 to cilia is regulated by Importin
615 $\beta 2$. *Journal of cell science*. 2011 Jan 1;jcs-070839.
616
- 617 Jenkins PM, Hurd TW, Zhang L, McEwen DP, Brown RL, Margolis B, Verhey KJ, Martens JR.
618 Ciliary targeting of olfactory CNG channels requires the CNGB1b subunit and the kinesin-2 motor
619 protein, KIF17. *Current biology*. 2006 Jun 20;16(12):1211-6
620
- 621 Jimbo T, Kawasaki Y, Koyama R, Sato R, Takada S, Haraguchi K, Akiyama T. Identification of a
622 link between the tumour suppressor APC and the kinesin superfamily. *Nature cell biology*. 2002
623 Apr;4(4):323.
624
- 625 Johnson CA, Malicki JJ. The Nuclear Arsenal of Cilia. *Developmental cell*. 2019 Apr
626 22;49(2):161-70.
627
- 628 Kee HL, Dishinger JF, Blasius TL, Liu CJ, Margolis B, Verhey KJ. A size-exclusion permeability
629 barrier and nucleoporins characterize a ciliary pore complex that regulates transport into cilia.
630 *Nature cell biology*. 2012 Apr;14(4):431
631
- 632 Kozminski KG, Beech PL, Rosenbaum JL. The *Chlamydomonas* kinesin-like protein FLA10 is
633 involved in motility associated with the flagellar membrane. *The Journal of cell biology*. 1995 Dec
634 15;131(6):1517-27
635
- 636 Lange A, Mills RE, Lange CJ, Stewart M, Devine SE, Corbett AH. Classical nuclear localization
637 signals: definition, function, and interaction with importin α . *Journal of Biological Chemistry*. 2007
638 Feb 23;282(8):5101-5
639
- 640 Lee BJ, Cansizoglu AE, Süel KE, Louis TH, Zhang Z, Chook YM. Rules for nuclear localization
641 sequence recognition by karyopherin $\beta 2$. *Cell*. 2006 Aug 11;126(3):543-58
642
- 643 Le Bot N, Antony C, White J, Karsenti E, Vernos I. Role of xklp3, a subunit of the *Xenopus* kinesin
644 II heterotrimeric complex, in membrane transport between the endoplasmic reticulum and the
645 Golgi apparatus. *The Journal of cell biology*. 1998 Dec 14;143(6):1559-73.
646
- 647 Li L, Tian G, Peng H, Meng D, Wang L, Hu X, Tian C, He M, Zhou J, Chen L, Fu C. New class
648 of transcription factors controls ciliary assembly by recruiting RNA polymerase II in
649 *Chlamydomonas*. *Proceedings of the National Academy of Sciences*. 2018 Apr
650 24;115(17):4435-40
651
- 652 Lounsbury KM, Richards SA, Carey KL, Macara IG. Mutations within the Ran/TC4 GTPase
653 Effects on regulatory factor interactions and subcellular localization. *Journal of Biological
654 Chemistry*. 1996 Dec 20;271(51):32834-41
655

- 656 Ludington WB, Wemmer KA, Lechtreck KF, Witman GB, Marshall WF. Avalanche-like behavior
657 in flagellar import. *Proceedings of the National Academy of Sciences*. 2013 Feb 14;201217354.
658
- 659 Macho B, Brancorsini S, Fimia GM, Setou M, Hirokawa N, Sassone-Corsi P. CREM-dependent
660 transcription in male germ cells controlled by a kinesin. *Science*. 2002 Dec 20;298(5602):2388-
661 90
662
- 663 Madugula V, Lu L. A ternary complex comprising transportin1, Rab8 and the ciliary targeting
664 signal directs proteins to ciliary membranes. *J Cell Sci*. 2016 Oct 15;129(20):3922-34.
665
- 666 Maiuri T, Woloshansky T, Xia J, Truant R. The huntingtin N17 domain is a multifunctional CRM1
667 and Ran-dependent nuclear and cilial export signal. *Human molecular genetics*. 2013 Apr
668 1;22(7):1383-94
669
- 670 Mazelova J, Astuto-Gribble L, Inoue H, Tam BM, Schonteich E, Prekeris R, Moritz OL, Randazzo
671 PA, Deretic D. Ciliary targeting motif VxPx directs assembly of a trafficking module through Arf4.
672 *The EMBO journal*. 2009 Feb 4;28(3):183-92
673
- 674 McClure-Begley TD, Klymkowsky MW. Nuclear roles for cilia-associated proteins. *Cilia*. 2017
675 Dec;6(1):8.
676
- 677 Mitchison HM, Valente EM. Motile and non-motile cilia in human pathology: from function to
678 phenotypes. *The Journal of pathology*. 2017 Jan;241(2):294-309.
679
- 680 Moore MS, Blobel G. The GTP-binding protein Ran/TC4 is required for protein import into the
681 nucleus. *Nature*. 1993 Oct;365(6447):66
682
- 683 Morris RL, Scholey JM. Heterotrimeric kinesin-II is required for the assembly of motile 9+ 2 ciliary
684 axonemes on sea urchin embryos. *The Journal of cell biology*. 1997 Sep 8;138(5):1009-22.
685
- 686 Morris RL, English CN, Lou JE, Dufort FJ, Nordberg J, Terasaki M, Hinkle B. Redistribution of the
687 kinesin-II subunit KAP from cilia to nuclei during the mitotic and ciliogenic cycles in sea urchin
688 embryos. *Developmental biology*. 2004 Oct 1;274(1):56-69.
689
- 690 Mueller J, Perrone CA, Bower R, Cole DG, Porter ME. The FLA3 KAP subunit is required for
691 localization of kinesin-2 to the site of flagellar assembly and processive anterograde intraflagellar
692 transport. *Molecular biology of the cell*. 2005 Mar 1;16(3):1341-54
693
- 694 Murawala P, Tripathi MM, Vyas P, Salunke A, Joseph J. Nup358 interacts with APC and plays a
695 role in cell polarization. *J Cell Sci*. 2009 Sep 1;122(17):3113-22
696
- 697 Nagata KI, Puls A, Futter C, Aspenstrom P, Schaefer E, Nakata T, Hirokawa N, Hall A. The
698 MAP kinase kinase kinase MLK2 co-localizes with activated JNK along microtubules and
699 associates with kinesin superfamily motor KIF3. *The EMBO journal*. 1998 Jan 1;17(1):149-58
700
- 701 Neumann N, Jeffares DC, Poole AM. Outsourcing the nucleus: nuclear pore complex genes are
702 no longer encoded in nucleomorph genomes. *Evolutionary Bioinformatics*. 2006
703 Jan;2:117693430600200023
704
- 705 Pazour GJ, Dickert BL, Witman GB. The DHC1b (DHC2) isoform of cytoplasmic dynein is required
706 for flagellar assembly. *The Journal of cell biology*. 1999 Feb 8;144(3):473-81.

707
708 Plotnikova OV, Pugacheva EN, Golemis EA. Primary cilia and the cell cycle. *Methods in cell*
709 *biology* 2009 Jan 1 (Vol. 94, pp. 137-160). Academic Press.
710
711 Porter ME, Bower R, Knott JA, Byrd P, Dentler W. Cytoplasmic dynein heavy chain 1b is required
712 for flagellar assembly in *Chlamydomonas*. *Molecular biology of the cell*. 1999 Mar 1;10(3):693-
713 712.
714
715 Rosenbaum JL, Moulder JE, Ringo DL. Flagellar elongation and shortening in *Chlamydomonas*:
716 the use of cycloheximide and colchicine to study the synthesis and assembly of flagellar proteins.
717 *The Journal of cell biology*. 1969 May 1;41(2):600-19.
718
719 Rosenbaum JL, Witman GB. Intraflagellar transport. *Nature reviews Molecular cell biology*. 2002
720 Nov;3(11):813.
721
722 Sarpal R, Todi SV, Sivan-Loukianova E, Shirolkar S, Subramanian N, Raff EC, Erickson JW, Ray
723 K, Eberl DF. *Drosophila* KAP interacts with the kinesin II motor subunit KLP64D to assemble
724 chordotonal sensory cilia, but not sperm tails. *Current biology*. 2003 Sep 30;13(19):1687-96
725
726 Satir P, Satir BH. The conserved ancestral signaling pathway from cilium to nucleus. *Journal of*
727 *cell science*. 2019 Aug 1;132(15):jcs230441.
728
729 Seungoh LE, Eunyong LE, Hyunjin SH, Hwasun HA, Wonja CH, Wankee KI. Human kinesin
730 superfamily member 4 is dominantly localized in the nuclear matrix and is associated with
731 chromosomes during mitosis. *Biochemical Journal*. 2001 Dec 15;360(3):549-56.
732 Shimizu K, Kawabe H, Minami S, Honda T, Takaishi K, Shirataki H, Takai Y. SMAP, an Smg
733 GDS-associating protein having arm repeats and phosphorylated by Src tyrosine kinase.
734 *Journal of Biological Chemistry*. 1996 Oct 25;271(43):27013-7
735
736 Signor D, Wedaman KP, Orozco JT, Dwyer ND, Bargmann CI, Rose LS, Scholey JM. Role of a
737 class DHC1b dynein in retrograde transport of IFT motors and IFT raft particles along cilia, but
738 not dendrites, in chemosensory neurons of living *Caenorhabditis elegans*. *The Journal of cell*
739 *biology*. 1999 Nov 1;147(3):519-30.
740
741 Soderholm JF, Bird SL, Kalab P, Sampathkumar Y, Hasegawa K, Uehara-Bingen M, Weis K,
742 Heald R. Importazole, a small molecule inhibitor of the transport receptor importin- β . *ACS*
743 *chemical biology*. 2011 Apr 21;6(7):700-8
744
745 Soniat M, Chook YM. Karyopherin- β 2 recognition of a PY-NLS variant that lacks the proline-
746 tyrosine motif. *Structure*. 2016 Oct 4;24(10):1802-9
747
748 Stauber T, Simpson JC, Pepperkok R, Vernos I. A role for kinesin-2 in COPI-dependent recycling
749 between the ER and the Golgi complex. *Current biology*. 2006 Nov 21;16(22):2245-51.
750
751 Strambio-De-Castillia C, Niepel M, Rout MP. The nuclear pore complex: bridging nuclear
752 transport and gene regulation. *Nature reviews Molecular cell biology*. 2010 Jul;11(7):490.
753
754 Takao D, Dishinger JF, Kee HL, Pinskey JM, Allen BL, Verhey KJ. An assay for clogging the
755 ciliary pore complex distinguishes mechanisms of cytosolic and membrane protein entry. *Current*
756 *biology*. 2014 Oct 6;24(19):2288-94.
757

- 758 Takao D, Wang L, Boss A, Verhey KJ. Protein interaction analysis provides a map of the spatial
759 and temporal organization of the ciliary gating zone. *Current Biology*. 2017 Aug 7;27(15):2296-
760 306
- 761
- 762 Torrado B, Graña M, Badano JL, Irigoín F. Ciliary entry of the Hedgehog transcriptional activator
763 Gli2 is mediated by the nuclear import machinery but differs from nuclear transport in being Imp-
764 α/β 1-independent. *PLoS One*. 2016 Aug 31;11(8):e0162033.
- 765
- 766 Tenney A, Price M, Macatangay J, Hatt D, Kline T, Berezuk MA. Partial Characterization of an
767 Interaction between Kinesin Associated Protein 3 (Kap3) of Kinesin-2 and the Actin Cytoskeleton.
768 *Austin Biochem*. 2016;1(1):1003
- 769
- 770 Walther Z, Vashishtha M, Hall JL. The *Chlamydomonas* FLA10 gene encodes a novel kinesin-
771 homologous protein. *The Journal of cell biology*. 1994 Jul 1;126(1):175-88.
- 772
- 773 Wentz SR, Rout MP. The nuclear pore complex and nuclear transport. *Cold Spring Harbor*
774 *perspectives in biology*. 2010 Oct 1;2(10):a000562.
- 775
- 776 Witman GB, Carlson K, Berliner J, Rosenbaum JL. *Chlamydomonas* cilia: I. Isolation and
777 electrophoretic analysis of microtubules, matrix, membranes, and mastigonemes. *The Journal of*
778 *Cell Biology*. 1972 Sep 1;54(3):507-39.
- 779
- 780 Wood CR, Huang K, Diener DR, Rosenbaum JL. The cilium secretes bioactive ectosomes.
781 *Current Biology*. 2013 May 20;23(10):906-11.
- 782
- 783 Yamano T, Iguchi H, Fukuzawa H. Rapid transformation of *Chlamydomonas reinhardtii* without
784 cell-wall removal. *Journal of bioscience and bioengineering*. 2013 Jun 1;115(6):691-4
- 785
- 786 Zhao C, Omori Y, Brodowska K, Kovach P, Malicki J. Kinesin-2 family in vertebrate ciliogenesis.
787 *Proceedings of the National Academy of Sciences*. 2012 Feb 14;109(7):2388-93.
- 788
- 789 Zhu D, Zhong X, Tan R, Chen L, Huang G, Li J, Sun X, Xu L, Chen J, Ou Y, Zhang T. High-
790 throughput cloning of human liver complete open reading frames using homologous
791 recombination in *Escherichia coli*. *Analytical biochemistry*. 2010 Feb 15;397(2):162-7.

792
793

794 **Figure legends**

795
796

797 **Figure 1. Kinesin-associated protein KAP3 localizes in both the cilium and nucleus. A.** HA
798 -tagged KAP3A or KAP3B were transfected into hTERT-RPE cells. After 24 hours transfection,
799 cilium was induced under 0.25% serum starvation for another 24 hours. Cells were fixed with 4%
800 paraformaldehyde (PFA) and stained with rabbit anti-HA and mouse anti- α -tubulin antibodies.
801 **B.** HA-tagged KAP3A or KAP3B were expressed in non-ciliated COS-7 cells, After 24 hour
802 transfection, cells were fixed with 4% PFA and stained with anti-HA antibody. Cell nuclei are
803 pseudo-colored blue, following staining with DAPI. **C.** EGFP tagged KAP3A or KAP3B were
expressed in MDCK cells. **D.** Schematic illustration of EGFP tagged KAP3 truncated derivatives.

804 **E.** Western blotting analysis of the expression of EGFP tagged KAP3 transiently transfected
805 MDCK cells. **F.** Mapping the domains required for nuclear localization of KAP3A in MDCK cells:
806 a series of EGFP tagged KAP3A truncations were transfected into MDCK cells. 24 hours after
807 transfection, cells were fixed with 4% PFA and stained with mouse anti-HA antibody and DAPI.

808

809 **Figure 2. RanGTP regulates nuclear translocation of KAP3.** **A.** Dominant negative form of
810 Ran blocked nuclear localization of KAP3 in COS-7 cells. mCherry tagged wild-type Ran or GTP
811 bound dominant mutant RanQ69L were co-transfected with EGFP-KAP3 into COS-7 cells. After
812 24 h transfection, cells were fixed with 4% PFA and stained with anti-EGFP antibody and DAPI
813 **B.** Mapping the domains within KAP3 that is mediated by RanGTP mediated nuclear import. a
814 series of EGFP tagged KAP3 truncations were co- transfected with GTP-locked Ran mutant Q69L
815 into COS-7 cells. After 24 h transfection, cells were fixed with 4% PFA and stained with anti-EGFP
816 antibody and DAPI.

817

818 **Figure 3. Armadillo repeat domain 6-9 targets KAP3 to the ciliary base.** **A.** Schematic
819 illustration of full-length human KAP3 and its truncated derivatives for analyzing ciliary targeting.
820 **B.** Ciliary base localization of KAP3 truncations in hTERT-RPE cells. hTERT-RPE cells were
821 transfected with various truncated constructs of KAP3. After 24 h transfection, the cells suffered
822 serum starvation for cilium induction for another 24 hours and fixed with 4% PFA and co-stained
823 with mouse anti-acetylated α -tubulin (red) and rabbit anti-EGFP antibodies (green). nuclei are
824 stained with DAPI (blue).

825

826 **Figure 4. Dominant negative Ran mutants reduced percent ciliation in hTERT-RPE cells.** **A.**
827 dominant negative Ran mutants blocked cilia formation in hTERT-RPE cells. The plasmids
828 expressing Ran mutant were transfected into hTERT-RPE cells. 24 h after transfection, Cilium
829 was induced via serum starvation for another 24 h. The cells were fixed and labeled for acetylated
830 α -tubulin and nuclei are stained with DAPI. **B.** hTERT-RPE cells expressing dominant Ran mutant
831 reduced the percentage of ciliated cells. **C.** Quantification of cilia length. Data are presented as
832 the mean \pm SEM. The unpaired *t*-test analysis was performed. *P*-value of great than 0.05 was
833 considered no significant difference. The experiment was repeated three times. **D.** Localization of
834 IFT81 and KAP3 in ciliated hTERT-RPE cells expressing RanQ69L. Cilium was induced in
835 hTERT-RPE cells expressing RanQ69L via serum starvation. The cells were fixed and co-stained
836 with acetylated α -tubulin and IFT81, or KAP3 and Cep164. Nuclei are stained with DAPI.

837

838 **Figure 5. Inhibition of RanGTP function shortens cilia length and blocks ciliary trafficking**
839 **of KAP under steady-state conditions in *Chlamydomonas*.** **A.** Dose dependent inhibition of
840 cilia length by the small molecular inhibitor IPZ, which disrupts RanGTP interacting with importin
841 β . CC125 cells were treated with different concentration of IPZ for 120 min, fixed with 1%
842 glutaraldehyde, and imaged by DIC microscope at 40 \times magnification. **B.** Quantification of cilia
843 length. The unpaired *t*-test analysis was performed. *P*-value of less than 0.05 was considered
844 significant difference. **C.** Expression of the dominant negative mutant Ran1Q73L, corresponding
845 to human RanQ69L, exhibits either clumpy cells or shortened ciliary length in *Chlamydomonas*.
846 Linearized expression plasmid pChlamy-4-Ran1Q73L was transformed into CC-125 cells and
847 initially screened by colony PCR. The expression of Ran1Q73L was finally detected by western
848 blotting analysis via V5 antibody. Due to cleavage efficiency of 2A peptide in *Chlamydomonas*,
849 Ran1Q73L was existed in two forms: Ran1Q73L (correctly processed, green arrow) and Ble-2A-
850 Ran1Q73L (fused with the selection marker, red arrow). Asterisk indicates that the negative
851 control merely expresses zeocin resistance gene Ble. The representative images for the control
852 Cells and Ran1Q73L expressing cells were shown. **D.**
853 Inhibiting of Ran function by IPZ reduced ciliary localization of KAP. KAP-GFP reporter cells are
854 treated with 20 μ M IPZ for 2 h, fixed with 100% methanol, and mounted with prolong gold anti-
855 fade mounting medium. Ciliary localization of KAP is dramatically reduced after IPZ treatment in
856 *Chlamydomonas*. **E.** Kymograph analysis indicates IPZ blocked ciliary entry of KAP. KAP-GFP
857 cells were treated with either DMSO or 50 μ M IPZ for 20 min, and then used for TIRF microscopy
858 to record the dynamic behavior of KAP.

859
860 **Figure 6. RanGTP directly regulates ciliary protein incorporation in *Chlamydomonas***
861 **during ciliary regeneration** **A.** Possible models of incorporation of existing ciliary protein into
862 cilia after treated with cycloheximide (CHX) and importazole (IPZ) during ciliary regeneration.
863 Inhibition of new protein synthesis by CHX results in half-length cilia. **B.** Wild-type CC-125 cells
864 were deciliated, and cilia were regenerated for 1 hour in the presence of different small
865 molecular inhibitors: 10 μ g/mL CHX, 10 μ M IPZ or the combination of 10 μ g/mL CHX and 10 μ M
866 IPZ. Cells were fixed with 1% glutaraldehyde and imaged by DIC microscope at
867 40 \times magnification. **C.** Schematic representation of IPZ washout assay under the absence of
868 newly synthesized protein. **D.** Deciliated cells were treated with the combination of 10 μ g/mL
869 CHX and 10 μ M IPZ for 60 min. Then IPZ, not CHX, was washed out, and cilia were
870 regenerated for other 60 min. Cells were fixed with 1% glutaraldehyde and cilia length was
871 measured using ImageJ software.

872

873 **Figure S1. Nuclear translocation of KAP3 is transport receptor importin β 2 independent. A.**

874 Importin β 2 mediates nuclear translocation of hnRNP A1. The plasmid myc-MBP-M9M expressing
875 myc-MBP fused inhibitory peptide M9M of importin β 2, or its control merely expressing myc-MBP,
876 was transfected into COS-7 cells. 24 hours after transfection, cells were fixed with 4% PFA and
877 co-stained with rabbit anti-myc (Red) and mouse anti-hnRNP A1 antibodies (green). nuclei are
878 stained with DAPI (blue). **B.** Importin β 2 isn't required for nuclear localization of KAP3. Importin
879 β 2 mediates nuclear translocation of hnRNP A1. The plasmid myc-MBP-M9M or its control was
880 co-transfected with EGFP-KAP3 into COS-7 cells. 24 hours after transfection, cells were fixed
881 with 4% PFA and co-stained with mouse anti-myc (Red) and rabbit anti-EGFP antibodies (green).
882 nuclei are stained with DAPI (blue).

883

884 **Figure S2. Subcellular localization of wild-type Ran and its dominant negative mutants in**

885 **serum starved hTERT-RPE cells.** Plasmids for expressing wild-type Ran or its point mutants
886 (RanQ69L, RanG19V and RanT24N) were transfected into hTERT-RPE cells. After 24 h
887 transfection, the cells were suffered for serum starvation for another 24 h, and then fixed with 4%
888 PFA. The intracellular localization of these proteins was visualized via immunofluorescence
889 staining.

890

891 **Figure S3. Alignment of human Ran with *Chlamydomonas* Ran like small GTPase (Ran1).**

892 Human Ran (NCBI reference sequence: NP_006316.1) and *Chlamydomonas* Ran1 (Phytozome
893 reference sequence: cre03.g191050.t1.2) were aligned using the Clustal Omega software.
894 Conserved residues are indicated (asterisk indicates fully conserved residues; colon indicates
895 residues with strongly similar properties; period indicates residues with weakly similar
896 properties). The key residues required for GTP or GDP bound state of Ran are marked in red.

897

898 **Figure S4. RanGTP regulates ciliary protein incorporation in *Chlamydomonas* regardless of the**

899 **presence of new synthesized proteins. A.** Possible models for RanGTP regulating ciliary protein
900 incorporation in the presence of new synthesized proteins. **B.** Deciliated cells were treated 10
901 μ M IPZ for 60 min. Then IPZ was washed and cilia were regenerated for another 60 min. Cells
902 were fixed with 1% glutaraldehyde and cilia length was measured using ImageJ software.

Figure 1

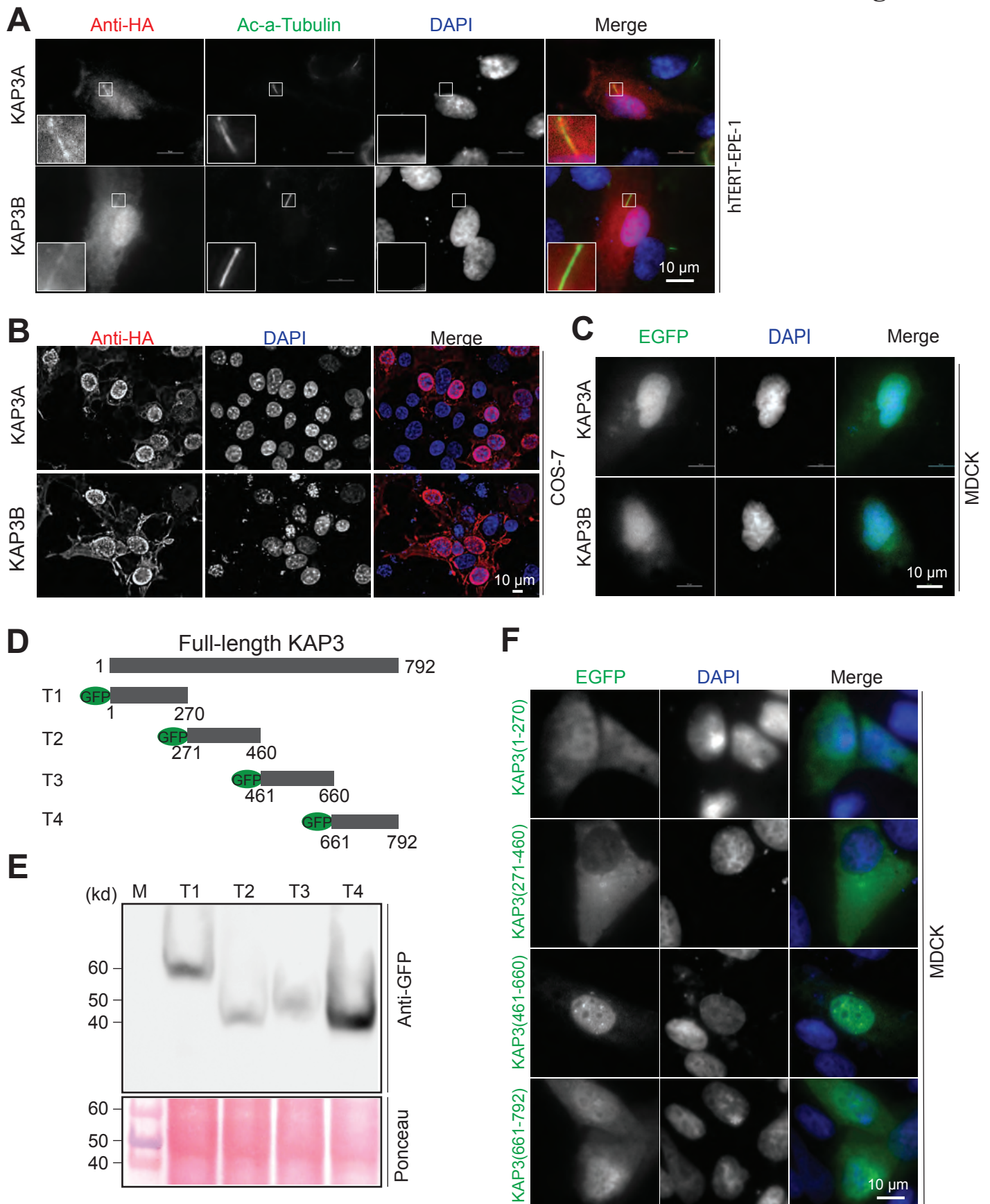


Figure 1. Kinesin-associated protein KAP3 localizes in both the cilium and nucleus

Figure 2

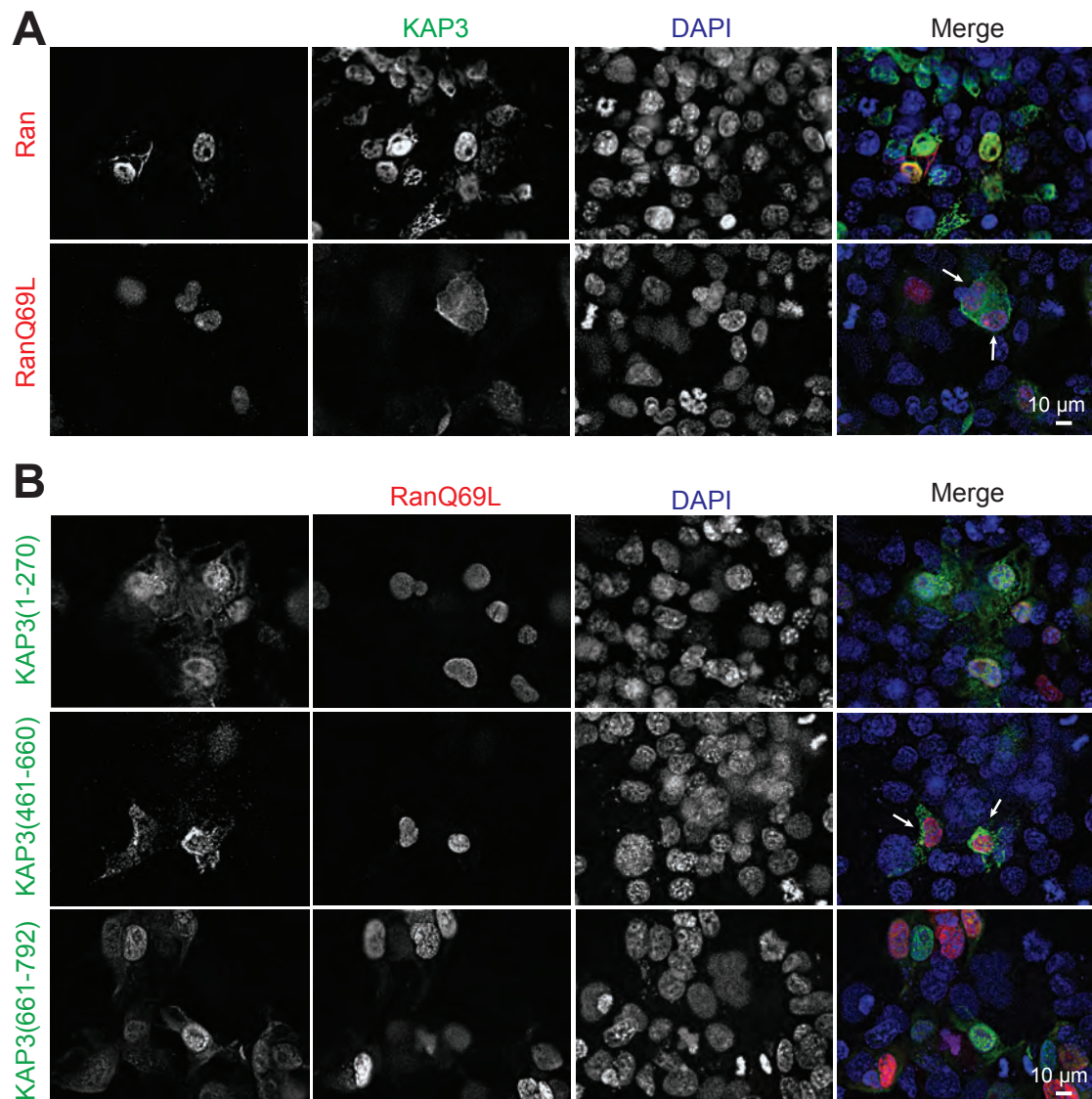


Figure 2. RanGTP regulates nuclear translocation of KAP3.

Figure 3

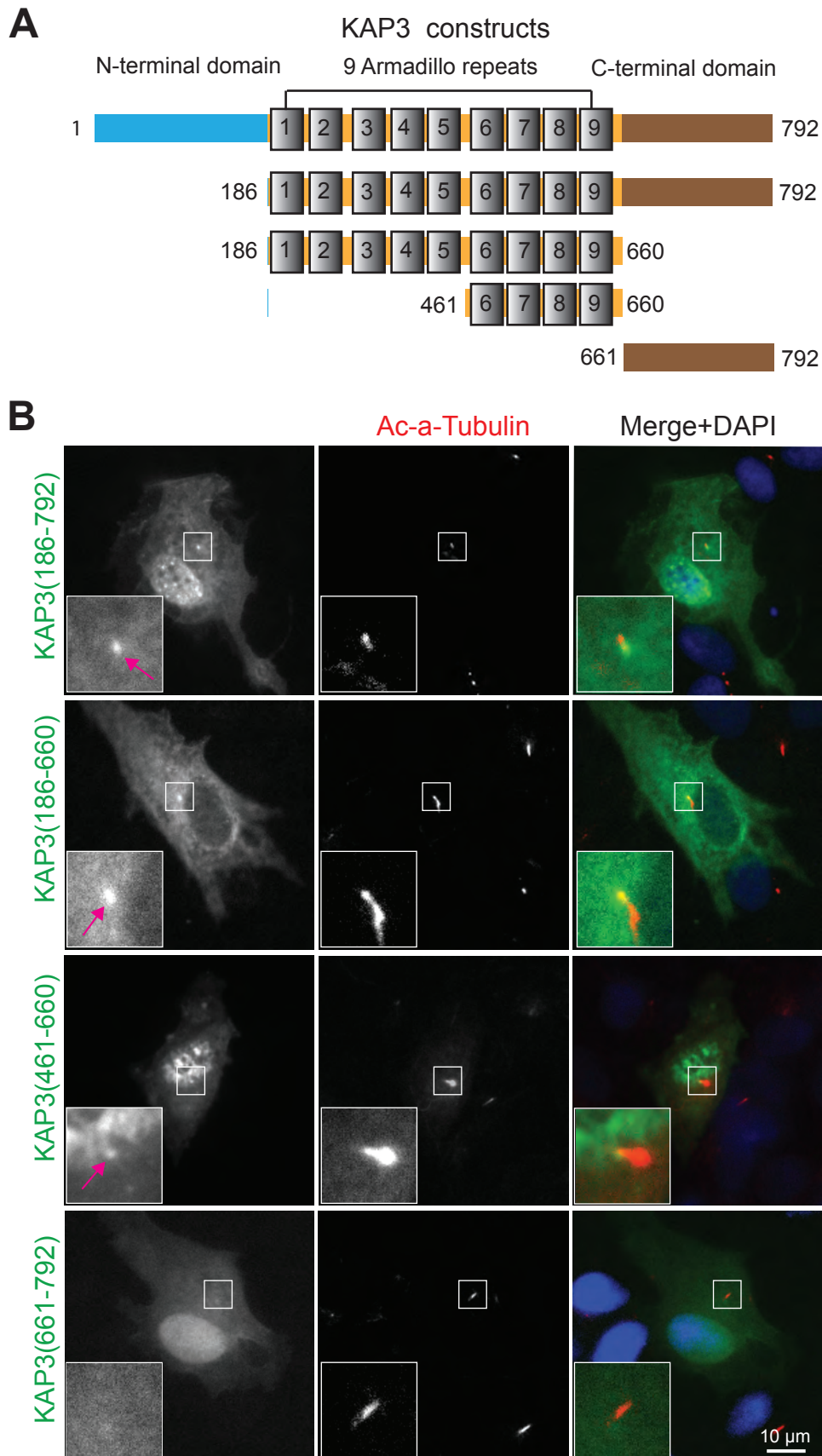


Figure 3. Armadillo repeat domain 6-9 targets KAP3 to the ciliary base

Figure 4

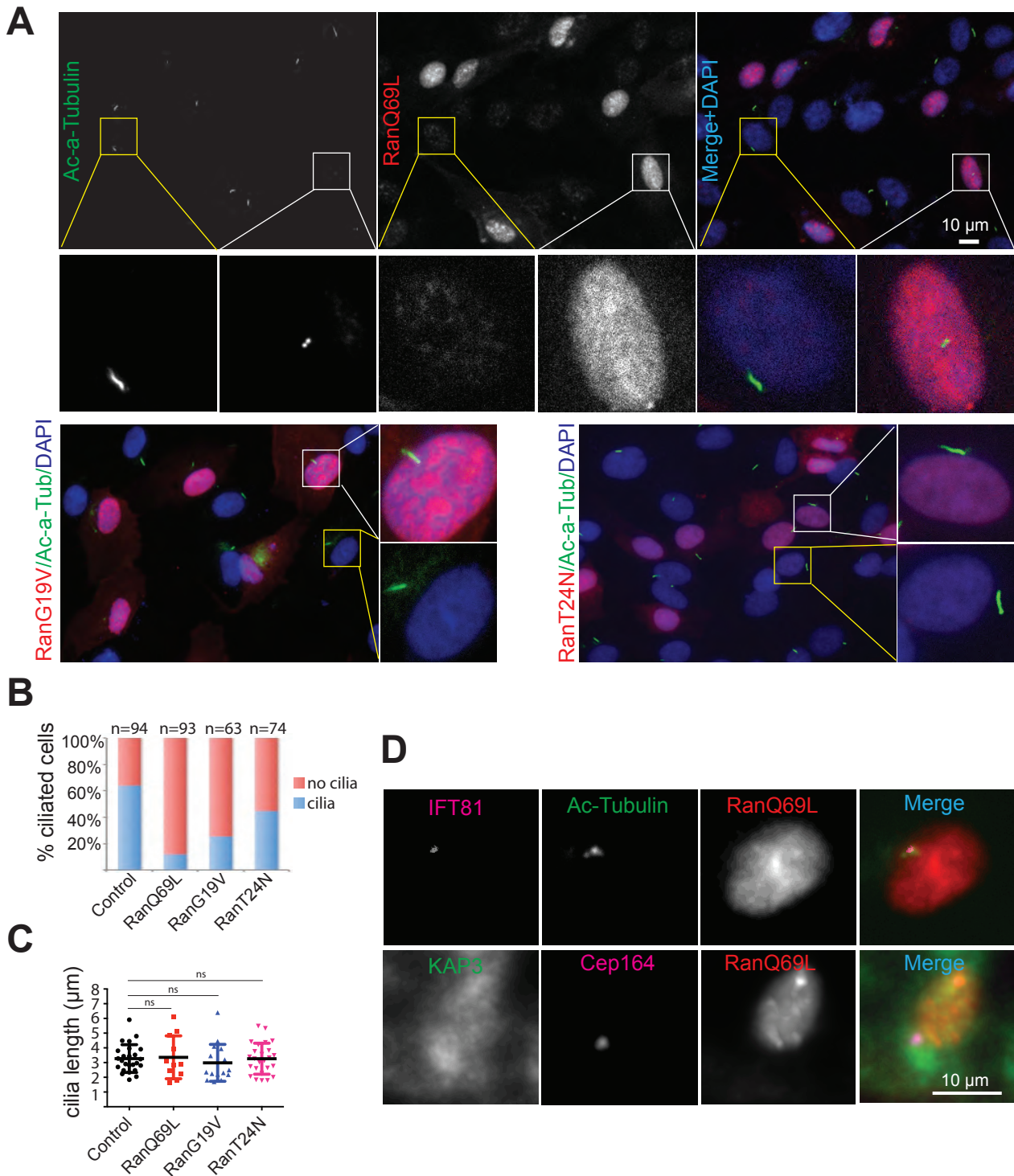


Figure 4. Dominant negative Ran mutants reduce percent ciliation in hTERT-RPE cells

Figure 5

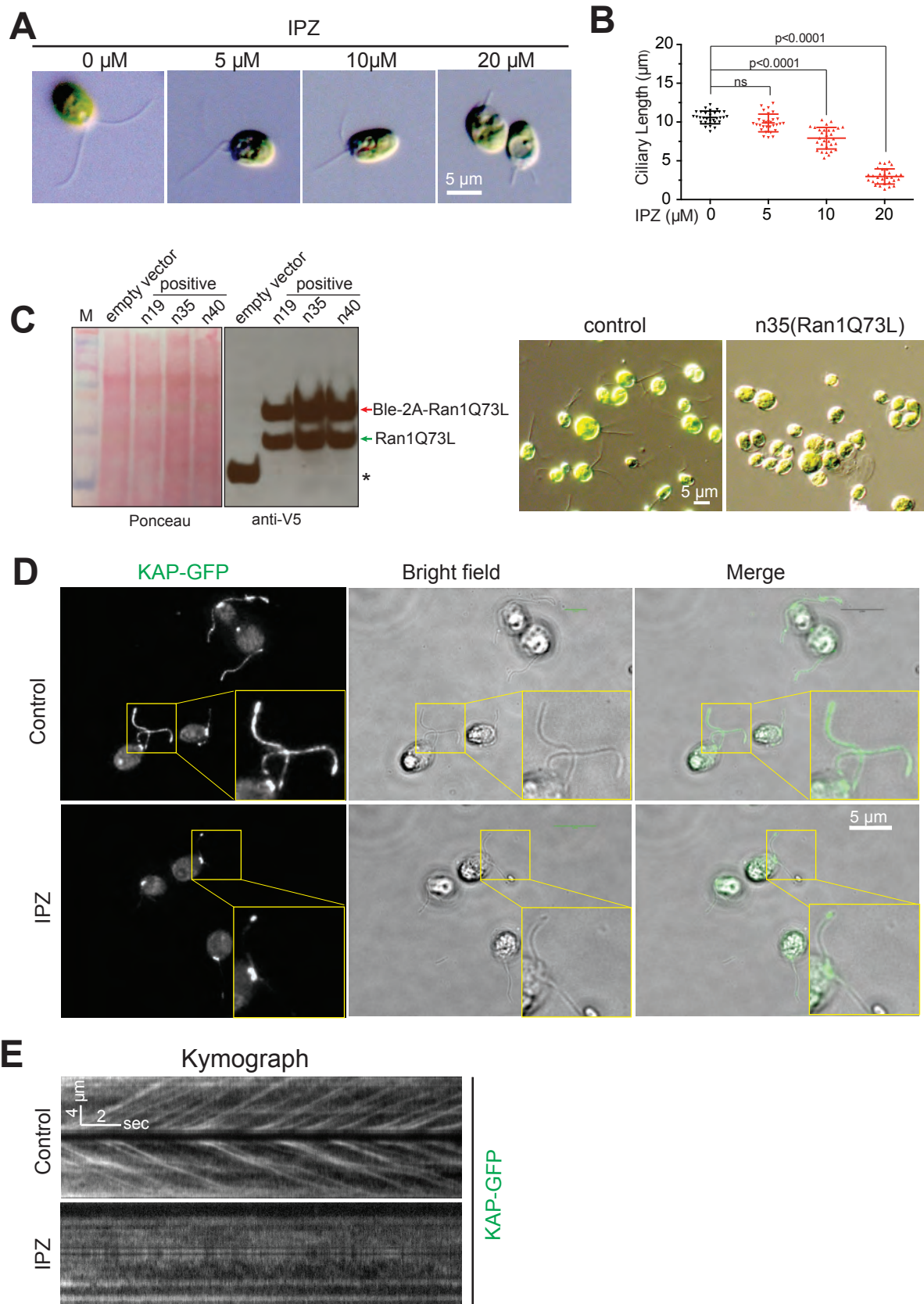


Figure 5. Inhibition of RanGTP function shortens cilia length and blocks ciliary trafficking of KAP under steady-state conditions in *Chlamydomonas*.

Figure 6

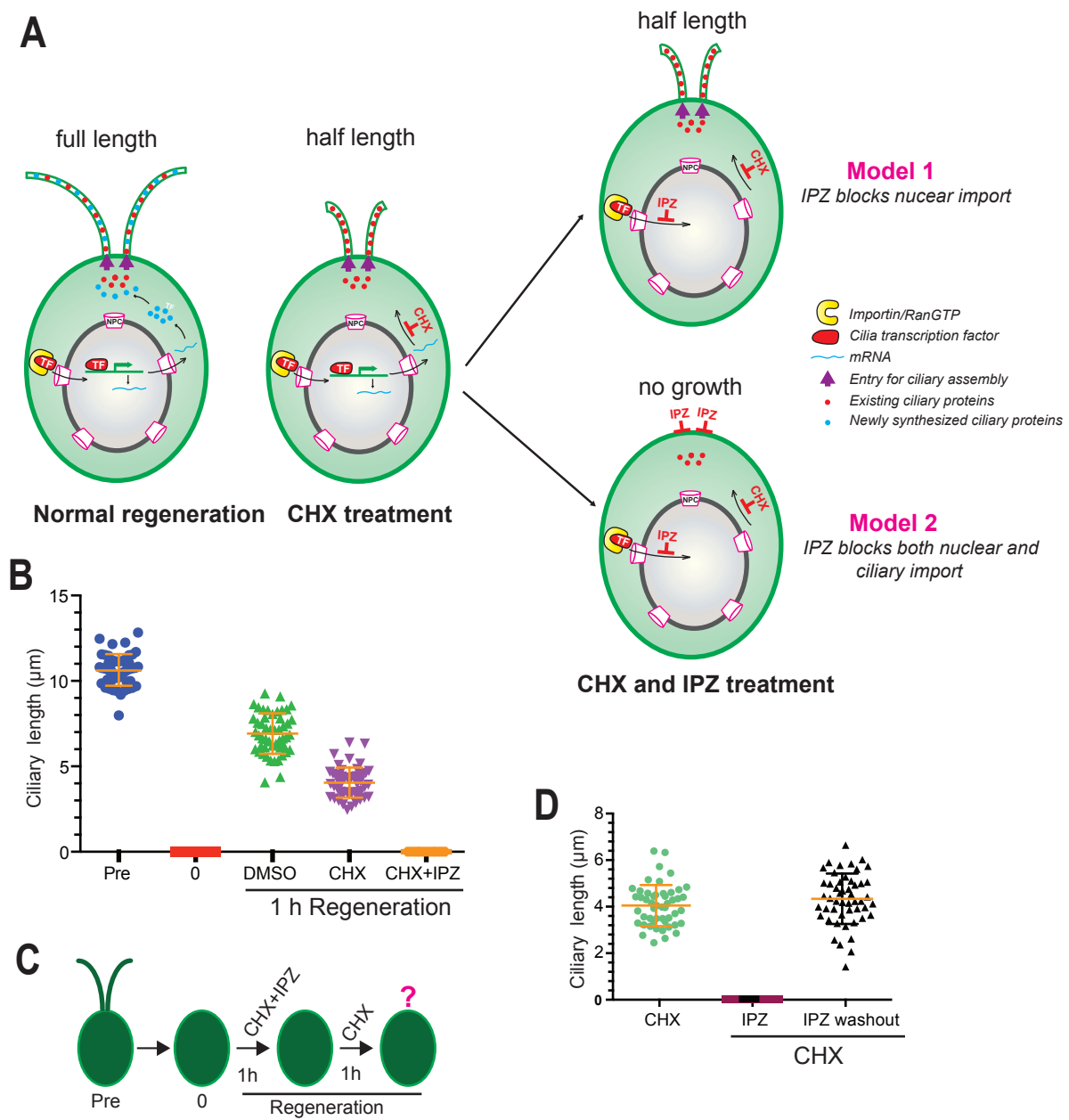


Figure 6. RanGTP directly regulates ciliary protein incorporation in *Chlamydomonas* during ciliary regeneration

Figure S1

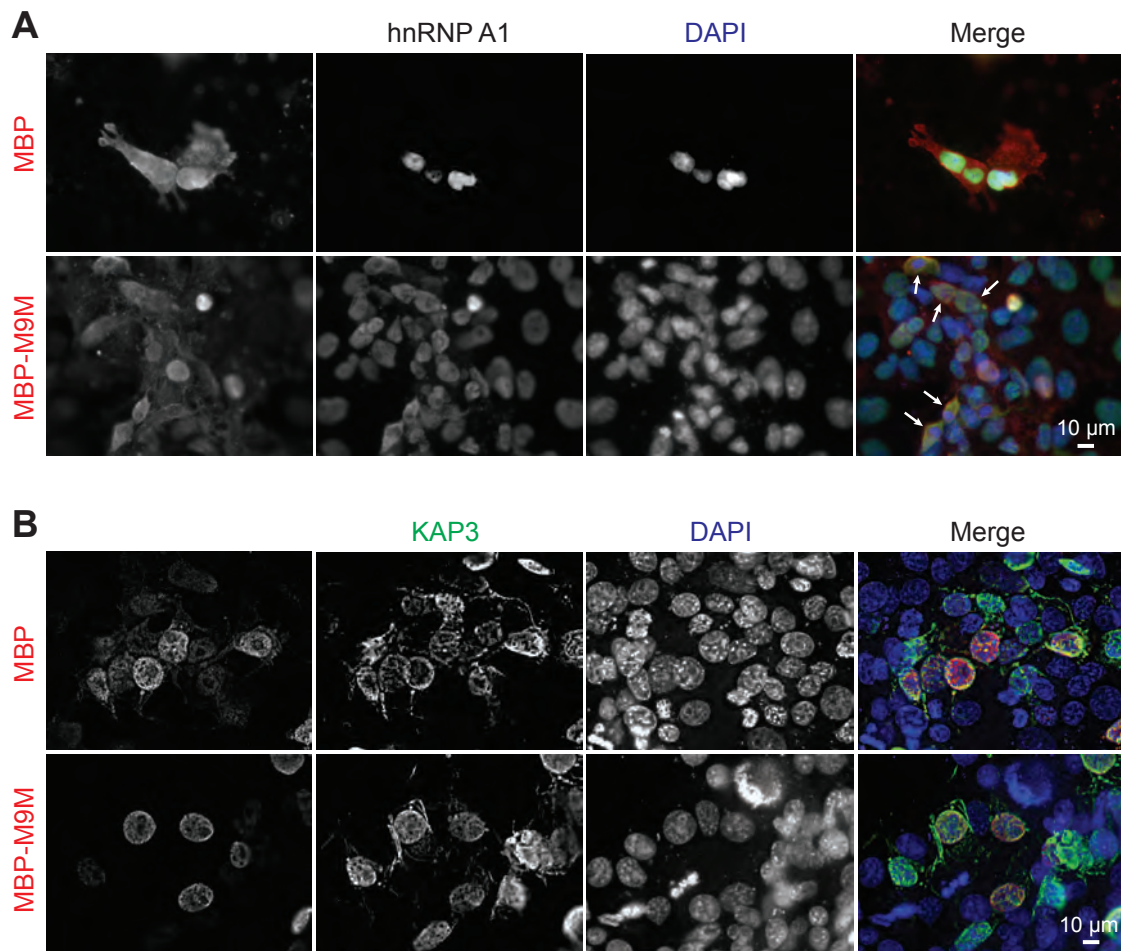


Figure S1. Nuclear translocation of KAP3 is transport receptor importin β 2 independent

Figure S2

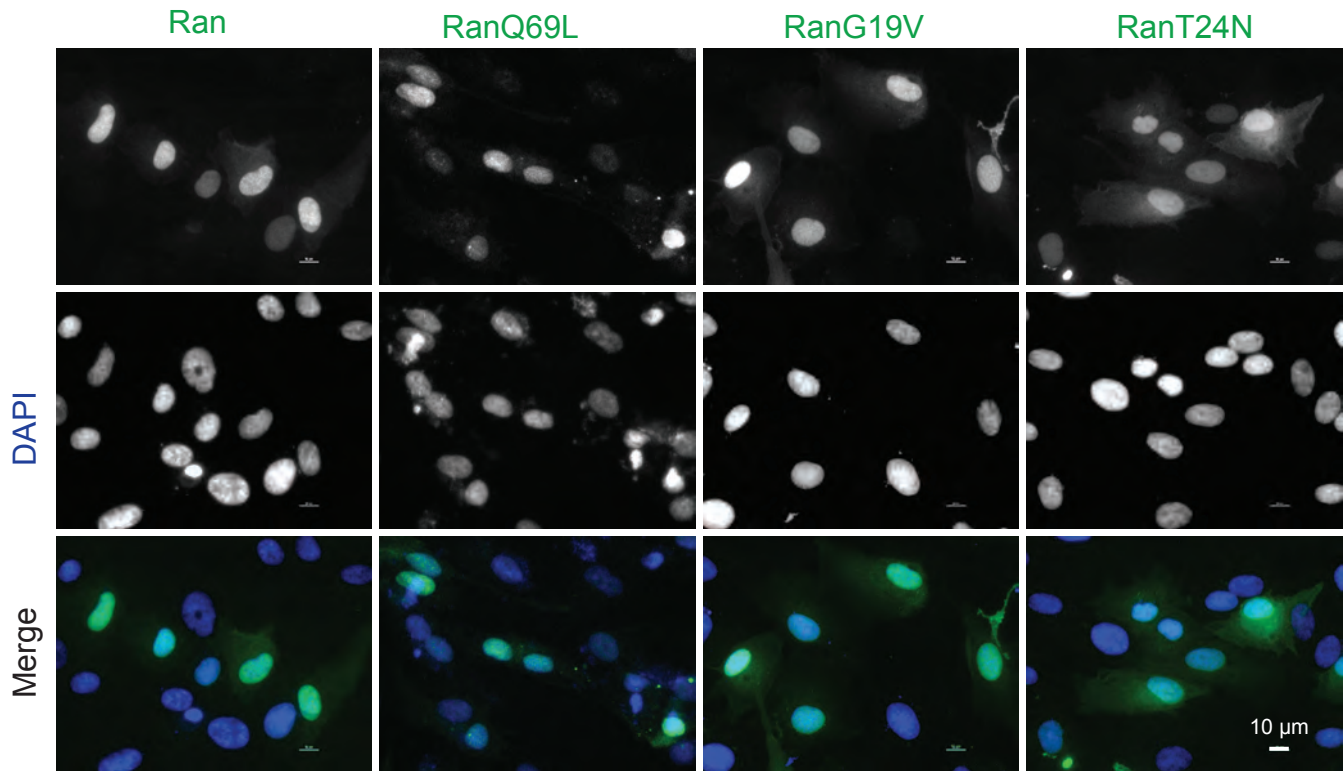


Figure S2. Subcellular localization of wild-type Ran and its dominant negative mutants in serum starved hTERT-RPE cells

Figure S3

```
human Ran  MA----AQGEPQVQFKLVLVGDGGTGKTTFFVKRHLTGEFEKKYVATLGVEVHPLVFHTNR 56
Chlamy Ran1 MALPGQTTPEGVPAFKLVLVGDGGTGKTTFFVKRHITGEFEKKYEPTIGVEVRPLDFTTNR 60
**      : *      *****:***** *:****:* * **

human Ran  GPIKFNVDWTAGQEKFGGLRDGYIQAQCAIIMFDVTSRVTYKNVFNWHRDLVRVCENIP 116
Chlamy Ran1 GKIRFYCWDWTAGQEKFGGLRDGYIHGQCAIIMFDVTSRLTYKNVPTWHRDLRCVCENIP 120
* *:* *****:*****:*****.***** *****

human Ran  IVLCGNKVDIKDRKVKAKSIVFHRKKNLQYYDISAKSNYNFEKPFLLWLRKLIIGDPNLEF 176
Chlamy Ran1 IVLCGNKVDVKNRQVKPKQVTFHRKKNLQYYEISAKSNYNYEKPFLLYLARKLTGDPHLSF 180
*****:*:*:* *.:.*****:*****:*****:***** **:*.*

human Ran  VAMPALAPPEVMDPALAAQYEHDLVAQTALPDEDDDL--- 216
Chlamy Ran1 VEEVALPPPEVQIDLAEQQRNEAELEQAAQQPLPADDDDELDD 223
* ** **** :* * : * :** * ** :***
```

Figure S3. Sequence alignment of human Ran with *Chlamydomonas* Ran like small GTPase (Ran1).

